Engineering pore-confined ultrafine Pt nanoparticles in hollow mesoporous carbon spheres for synergistically enhanced bifunctional electrocatalysis of sustainable hydrogen evolution and ethylene glycol oxidation

Man Zhao[‡, a], Jiamin Ma[‡,a], Ze Wang[a], Shuai He [a], Na Gao[a], Qinyun Yan[a], Liwu Qiang[a], Wei Wen[a], Lifang Shi[a], Junming Zhang[a], Xiaoli Li[b,*], He Xiao[a,*], Jianfeng Jia [a,*]

[a]Shanxi Center of Technology Innovation for Advanced Power Battery Material, School of Chemistry and Chemical Engineering, Shanxi Normal University, Taiyuan, 030000, China

[b]School of Materials Science and Engineering, Hebei University of Engineering, Handan 056038, China

*Corresponding author. E-mail: lixiaoli@hebei.edu.cn (Xiaoli Li); xiaohe200808@sxnu.edu.cn (He Xiao); jiajf@dns.sxnu.edu.cn (Jianfeng Jia).

Author contributions

[‡]These authors made equal contribution.

Experimental part

Calculation of Mass Activity

The mass activity (MA, in A mg^{-1}_{Pt}) was calculated to evaluate the utilization efficiency of platinum. The formula used is

$$MA = j/m_{Pt}$$

Where j is the current measured at a specific potential, and m_{Pt} is the mass loading of platinum only on the working electrode.

The Pt mass loading was determined as follows: First, the total catalyst loading on the electrode was 0.025mg (5 mg sample was dispersed in 500 μL dispersion, and 2.5 μL

was dipped in the glassy electrode). The Pt mass fraction in the catalyst (ω_{Pt}, in wt.%) was determined by ICP-OES (**Table S2**). Then the platinum loading was calculated as:

$$m_{Pt} = (\text{total catalyst loading}) \times (\omega_{Pt} / 100)$$

For example, for Pt/HMCs-10 with a total catalyst loading of 0.025 mg and a Pt content of 0.83 wt.%, m_{Pt} = 0.025 mg× 0.0083 = 0.2075 μg. This value was used for all mass activity normalizations. Crucially, the mass of the carbon support was excluded from this calculation.

Electrochemical measurement

The working electrode consists of a polished glassy carbon electrode (GCE, 3 mm diameter) modified with catalyst material. A graphite rod serves as the counter electrode, while either a saturated calomel electrode (SCE, filled with 0.5 M H_2SO_4) or Hg/HgO electrode (immersed in 1 M KOH) functions as the reference electrode, selected according to the electrolyte pH. For working electrode preparation, the GCE surface is first mechanically polished with α-Al_2O_3 slurry (20-50 nm particle size), followed by sequential ultrasonic cleaning in ethanol and deionized water (3 minutes each). The catalyst ink is prepared by homogenizing 5 mg of catalyst powder with 50 μL Nafion solution (5 wt%) in 500 μL of ethanol/water mixed solvent (1.25:1 v/v) through 30-minute ultrasonication. A precisely controlled 2.5 μL aliquot of the homogeneous ink is then drop-cast onto the pretreated GCE surface and air-dried.

Table S1 Textural parameters of HMCs-x and Pt/HMCs-x.

Sample	S_{BET} ($m^2 g^{-1}$)	V_{pore} ($cm^3 g^{-1}$)	Pore size (nm)
HMCs-5	1123.09	2.95	5.06
HMCs-10	1302.82	2.83	10.29
HMCs-15	1047.91	3.71	13.05
HMCs-20	1030.02	2.58	18.20
Pt/HMCs-5	872.81	1.74	6.21
Pt/HMCs-10	1096.07	2.15	13.14
Pt/HMCs-15	993.93	2.74	13.25
Pt/HMCs-20	851.74	2.45	19.77

Table S2 Calculated Pt^0 and Pt^{2+} content based on results of ICP-OES and XPS.

	Pt/HMCs-5	Pt/HMCs-10	Pt/HMCs-15	Pt/HMCs-20
Pt contents (%)	0.93	0.83	0.88	0.83
Pt^0 contents (%)	51.03	49.69	45.71	57.23
Pt^{2+} contents (%)	48.97	50.31	54.29	42.77

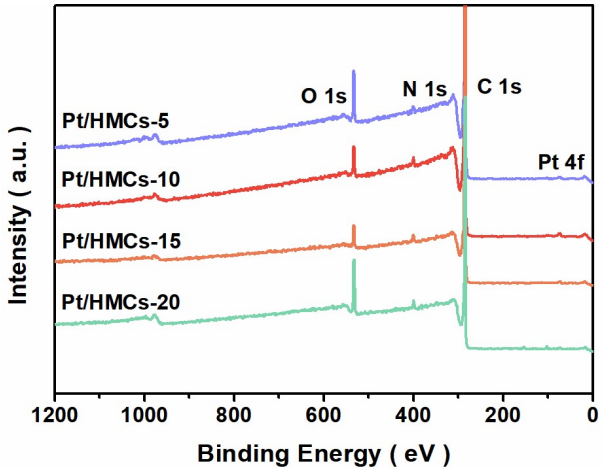

Fig. S1 XPS survey spectra of Pt/HMCs-x samples. The spectra confirm the presence of C, O, and Pt elements in all samples.

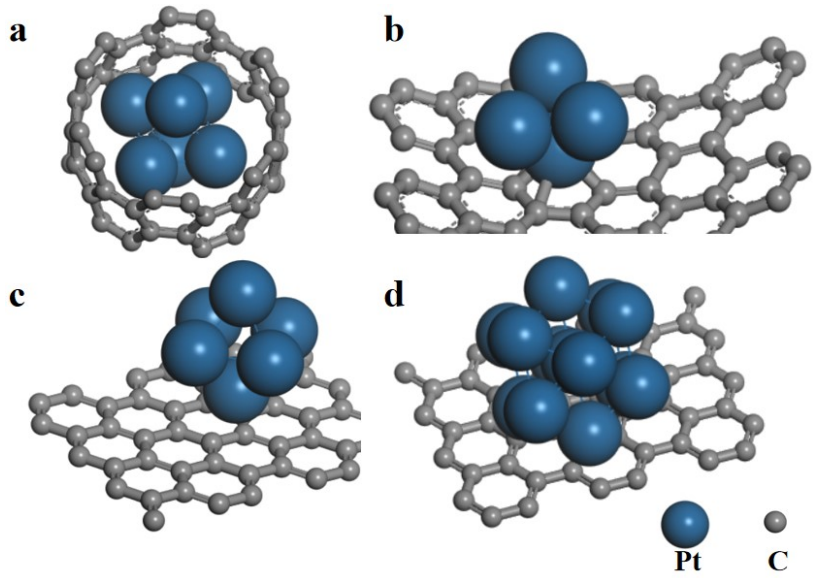

Fig. S2 The catalytic models of Pt-HMCs-5 (a), Pt-HMCs-10 (b), Pt-HMCs-15 (c), and Pt-HMCs-20 (d).

To further solidify our electronic structure interpretation, we performed density functional theory (DFT) calculations. Graphene sheets serve as the basic carbon support model, with curvature introduced to simulate pore size variations: high curvature mimics strong confinement (e.g., Pt/HMCs-5), while low curvature represents weak confinement (e.g., Pt/HMCs-20). Different Pt cluster sizes (e.g., Pt_4 for ~2.3 nm NPs and Pt_{13} for larger NPs) are employed to match experimentally observed size distributions. Calculations are performed using the VASP 5.4.4 package with key parameters including: PBE functional, 500 eV cutoff energy, 5×5×1 k-point grid for accurate sampling, and DFT-D3 correction to describe van der Waals interactions between Pt and the carbon support. Geometric optimization convergence criteria are set to atomic forces <0.02 eV/Å.

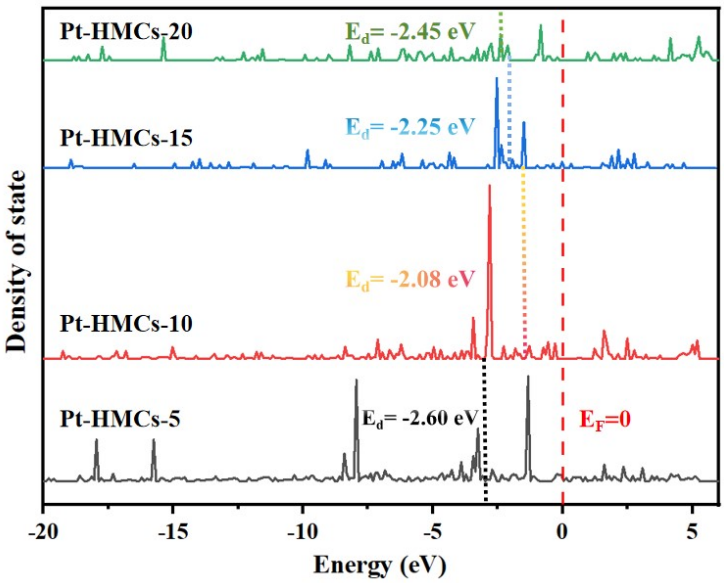

Fig. S3 Calculated Electronic Density of States (DOS) of Pt-HMCs-x Catalysts

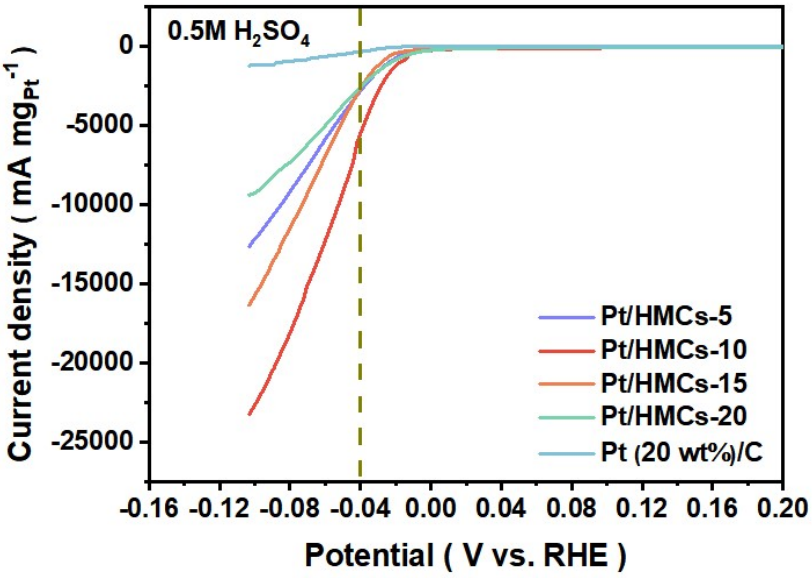

Fig. S4 HER LSV curves with iR compensation for all catalysts.

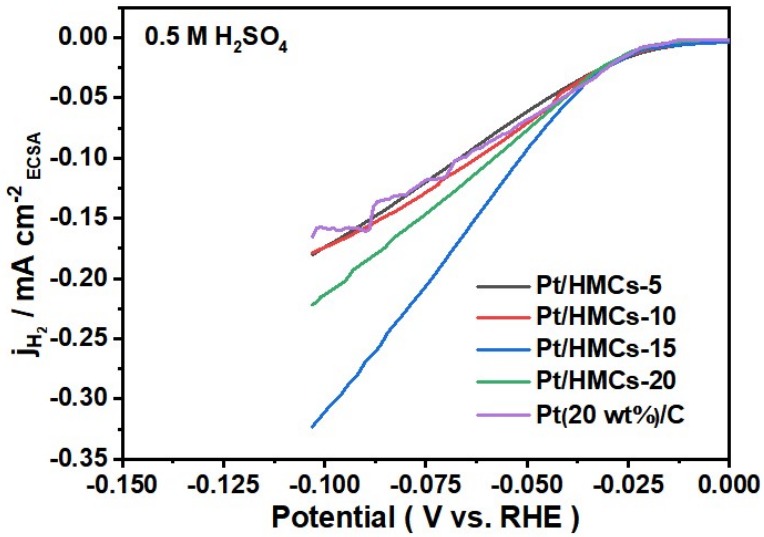

Fig. S5 HER specific activity (based on H-UPD ECSA) for all catalysts.

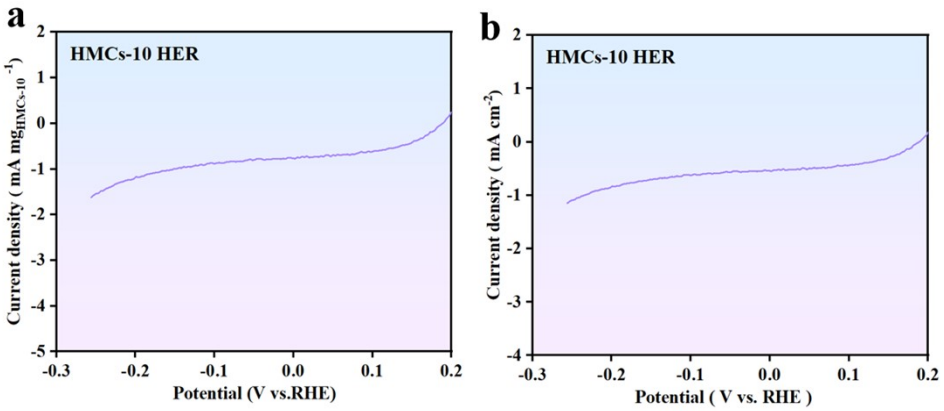

Fig. S6 LSV curve of HMCs-10 toward HER in 0.5 M H_2SO_4, the scan rate is 5 mV.

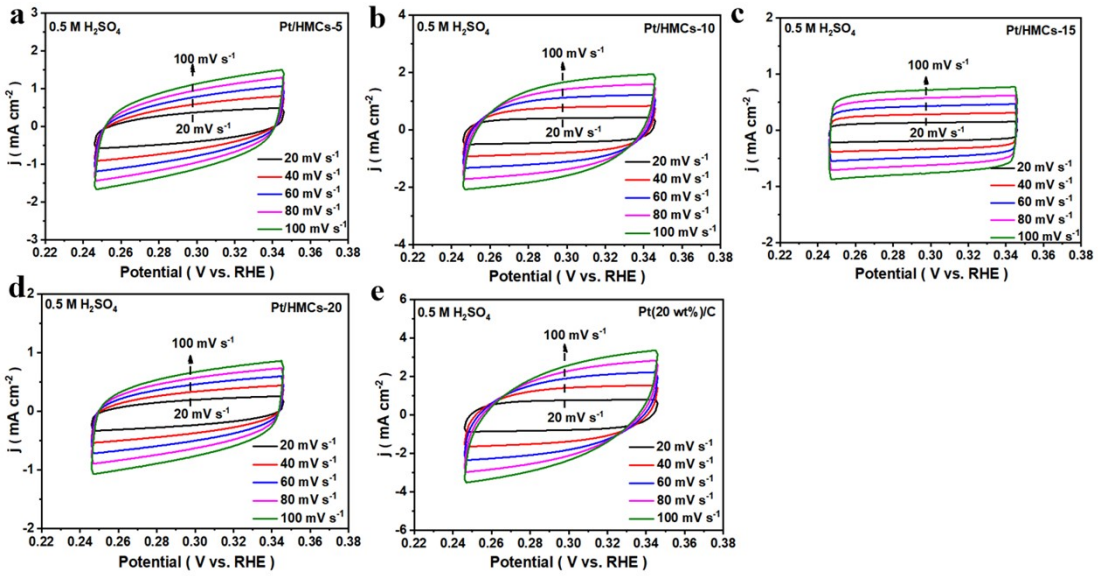

Fig. S7 CV curves of catalysts at scan rates from 20 to 100 mV s^{-1}. The CV curves were used for double-layer capacitance (Cdl) estimation for HER. CVs were recorded in the non-faradaic potential region of 0.22-0.38 V vs. RHE in 0.5 M H_2SO_4 electrolyte at varying scan rates (20, 40, 60, 80, and 100 mV s^{-1}). The current density is normalized to the geometric area of the glassy carbon electrode.

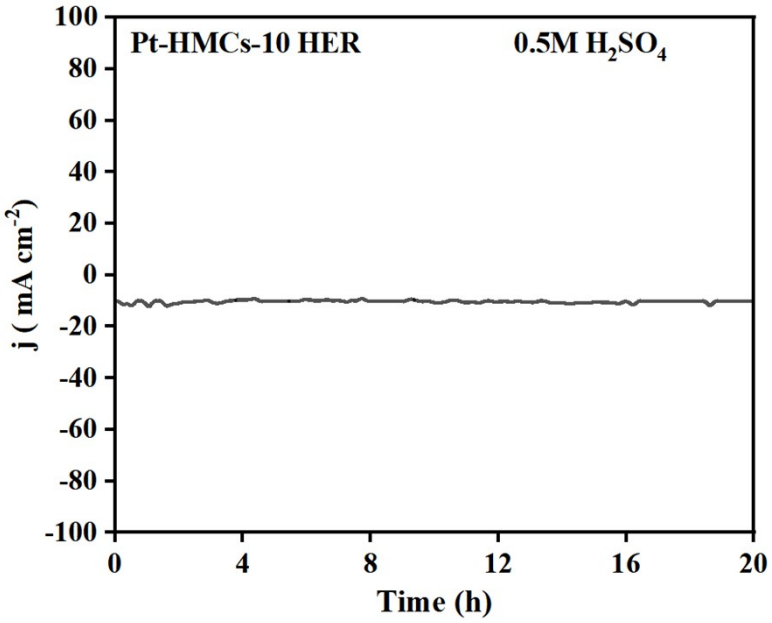

Fig.S8 I-t curves of HMCs-10 toward HER at a potential of -0.031V (vs. SHE)**.** The electrolyte is 0.5 M H_2SO_4.

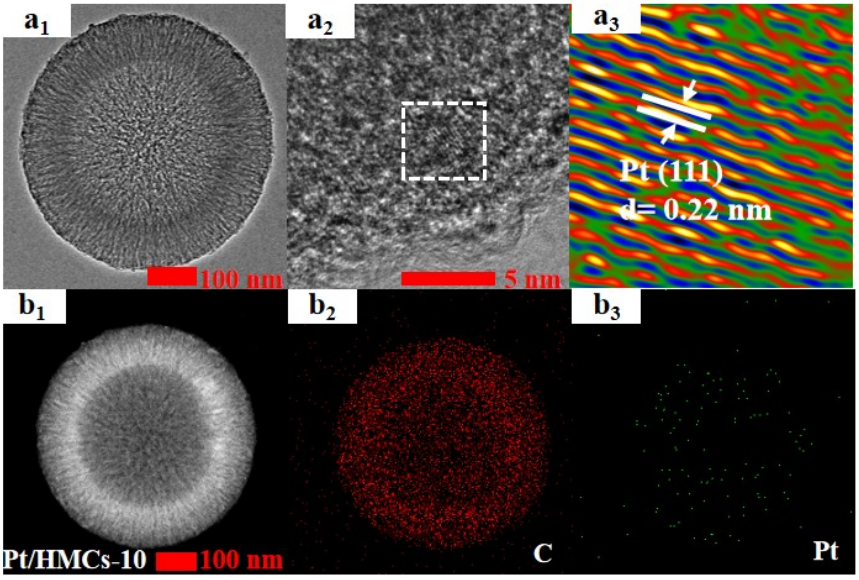

Fig. S9. (a_1) TEM image, (a_2) HRTEM image, and (a_3) corresponding lattice fringe image of Pt/HMCs-10 after 20 h of HER i-t testing; (b_1) HAADF-STEM image and (b_2, b_3) corresponding elemental mapping of Pt/HMCs-10 after 20 h of HER i-t testing.

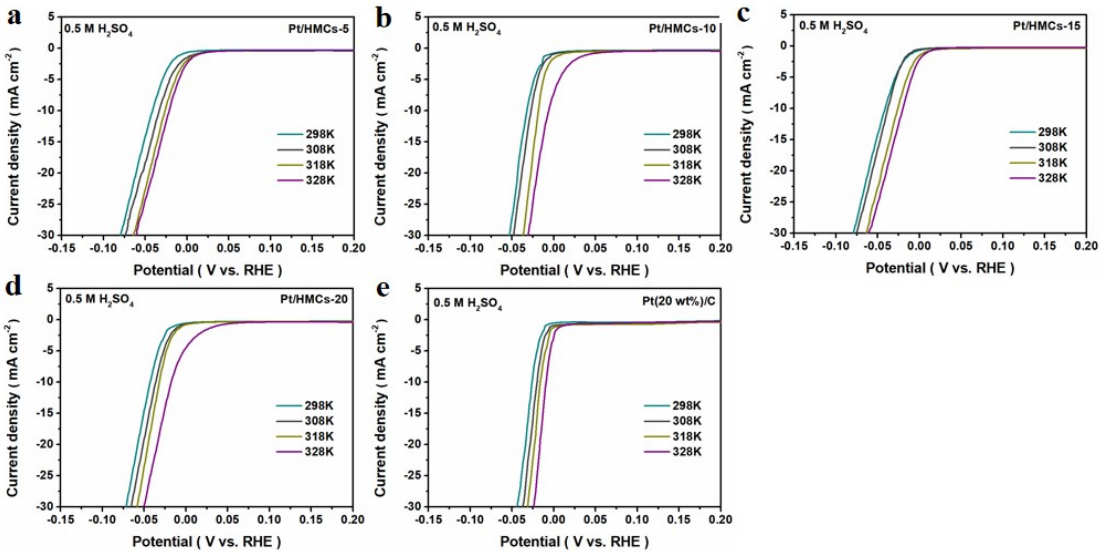

Fig. S10 LSV curves of as-prepared catalysts from 298 to 358 K for the HER in 0.5 M H_2SO_4 electrolyte, the scan rate is 5 $mV \cdot s^{-1}$.

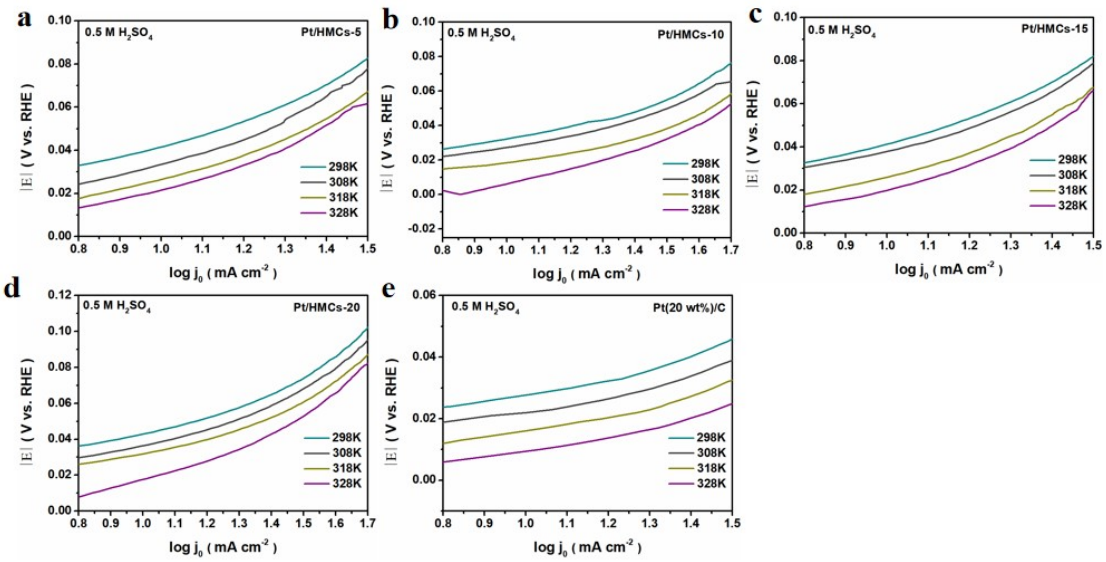

Fig. S11 Tafel curves of as-prepared catalysts from 298 to 348 K calculated from Fig.S10 for the HER.

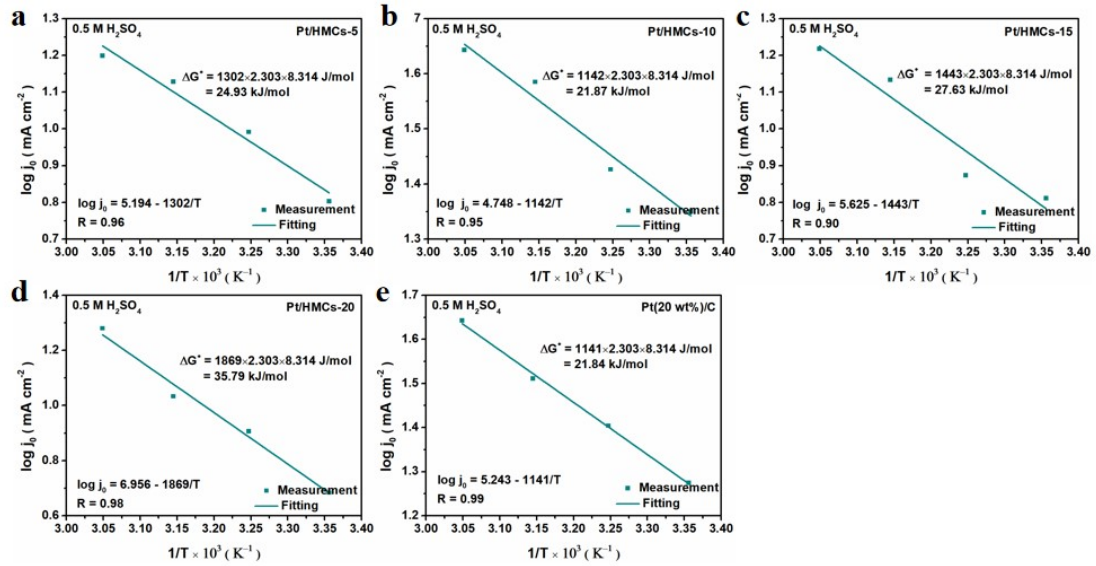

Fig. S12 Typical Arrhenius plots of as-prepared catalysts for the HER. The logarithm of the peak current density (log j~p~) from LSV curves is plotted against the inverse of temperature (1000/T). The linear fitting of the data allows for the activation free energy (ΔG^x).

Table S3. HER performance comparison with recently reported high-performance electrocatalysts.

Catalyst	Pt loading	Electrolyte	Mass activity	Activity	Stability	Reference
Pt1/OLC	0.27 wt%	0.5 M H_2SO_4	7.4 A mg^{-1} at -38 mV	38 mV at 10mA cm^{-2}	100 h 40mV	1
Pt1-MoS_2/hNCNC	3.76 wt%	0.5 M H_2SO_4	5.6 A mg^{-1} at -20 mV	11 mV at 10 mA cm^{-2}	100 h 50 mA cm^{-2}	2
Pt@MoS_2/NiS_2	1.8 at%	00.5 M H_2SO_4		34 mV at 10 mA cm^{-2}	72 h 50 mA cm^{-2}	3
s-Pt/1T'-MoS_2	10 wt%	1M $HClO_4$	85 A mg^{-1} -50mV	19 mV at 10 mA cm^{-2}	500 h 100 mA cm^{-2}	4
Pt-doped 1T-MoS_2	3 wt%	0.5 M H_2SO_4		140 mV at 10 mA cm^{-2}	1000cycles of CV	5
Pt-PVP/TNR@GC		0.5 M H_2SO_4	16.53 A mg^{-1} -50mV	21 mV at 10 mA cm^{-2}	44 h -0.021V	6
Pt1@PC	2.2 wt%	0.5 M H_2SO_4	12.7 A mg^{-1} -10mV	19 mV at 10 mA cm^{-2}	100 h 10 mA cm-2	7
Pt1/MC		0.5 M H_2SO_4	7.5 A mg^{-1} -50mV	25 mV at 10 mA cm^{-2}	10h	8
Pt/HMCs-10	0.83 wt%	0.5 M H_2SO_4	5.5 A mg^{-1}	33 mV at 10 mA cm-2	30 h	This work

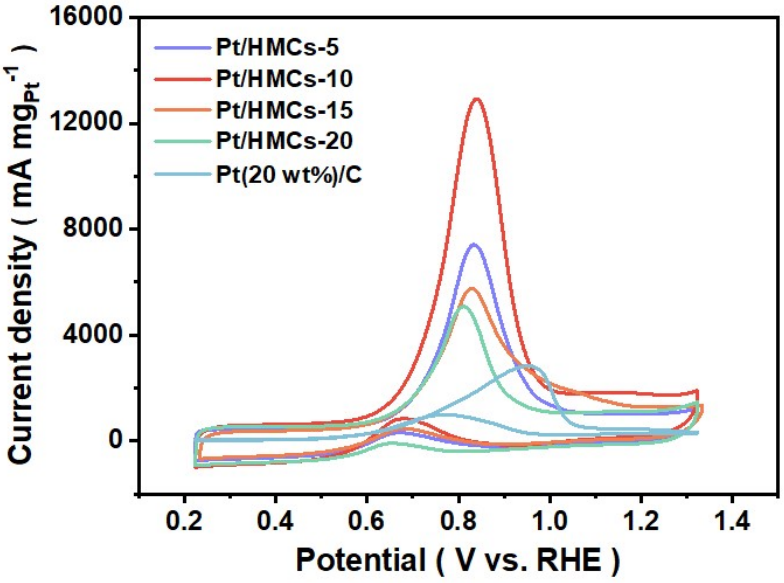

Fig. S13 EGOR CV curves with iR compensation for all catalysts.

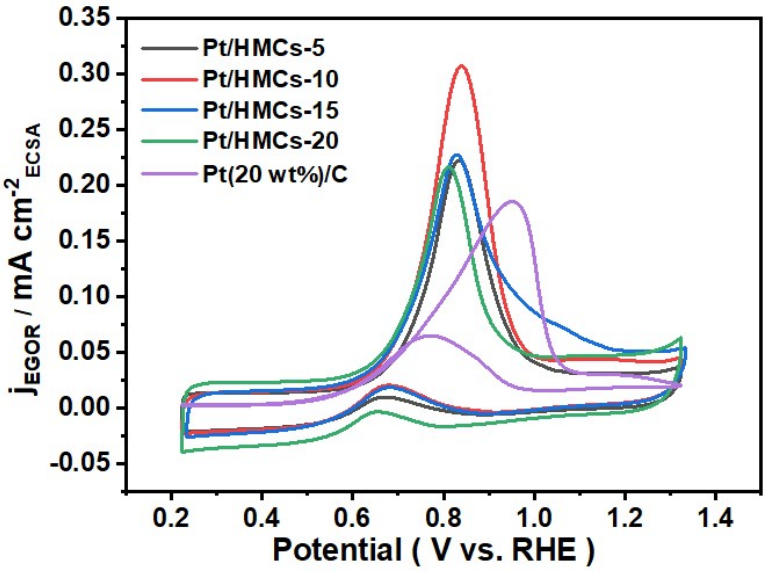

Fig. S14 EGOR C_{dl} normalized current density for all catalysts.

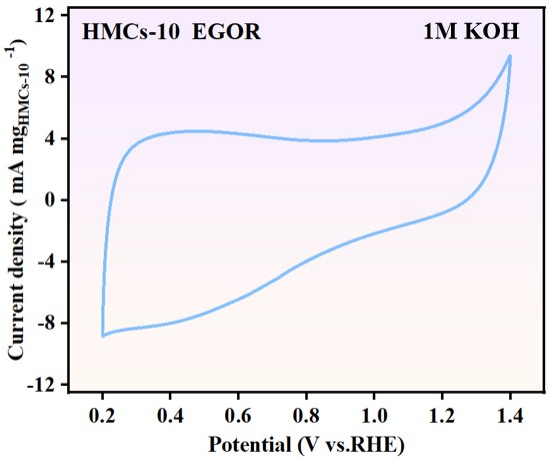

Fig. S15 CV curve of HMCs-10 toward EGOR in 1 M KOH + 1 M EG, the scan rate is 10 mV s^{-1}.

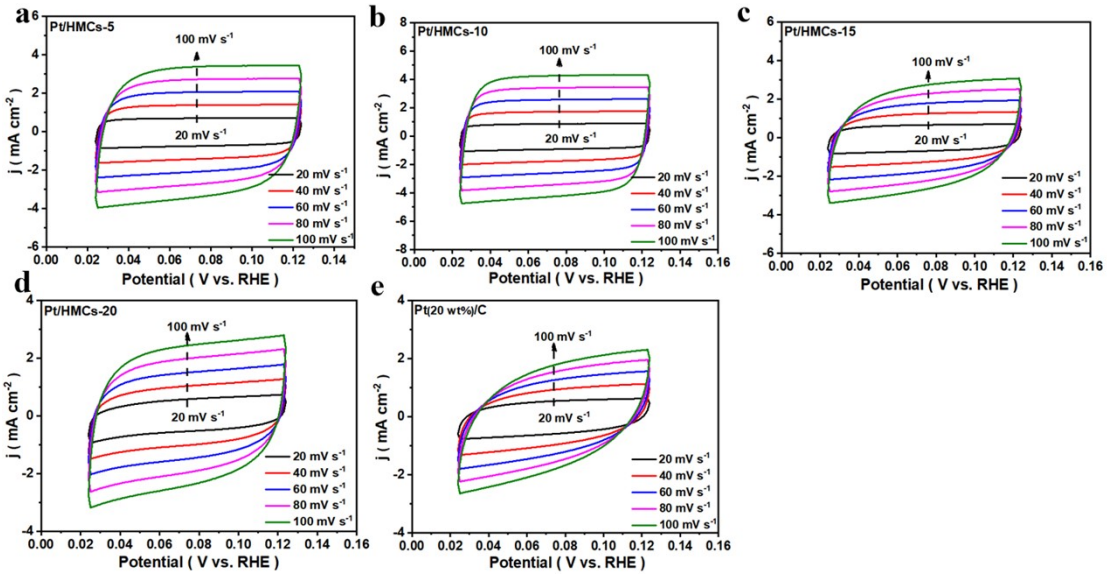

Fig. S16 CV curves of catalysts at scan rates from 20 to 100 mV s^{-1}. The CV curves were used for double-layer capacitance (C_{dl}) estimation for EGOR. CVs were recorded in the non-faradaic potential region of 0.00-0.16 V vs. RHE in in 1 M KOH with 1 M EG electrolyte at varying scan rates (20, 40, 60, 80, and 100 mV s^{-1}). The current density is normalized to the geometric area of the glassy carbon electrode.

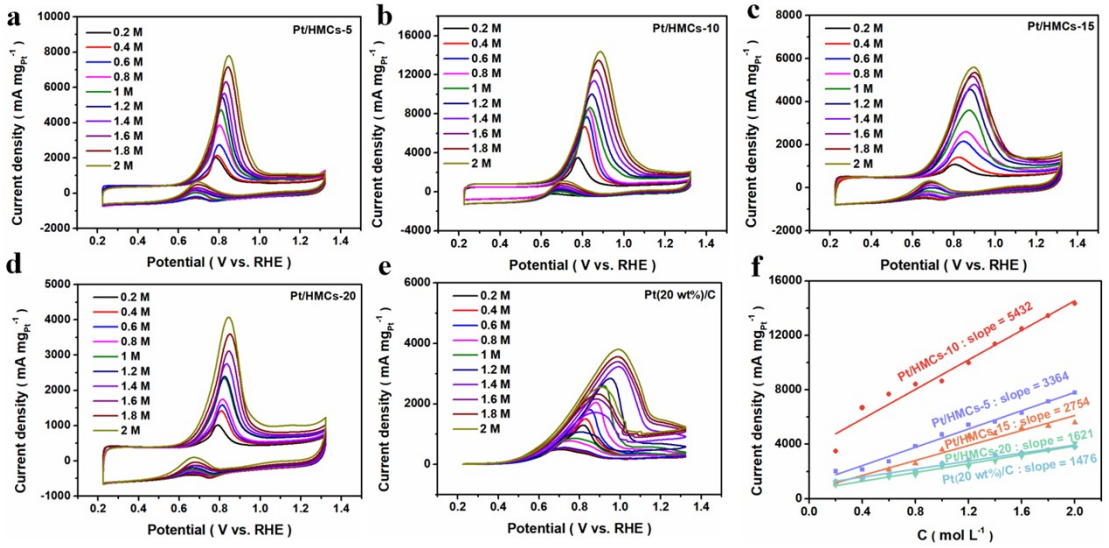

Fig. S17 CV curves of as-prepared catalysts at different EG concentrations toward EGOR recorded in 1 M KOH electrolyte at scan rates of 10 mV s^{-1}. The current density is normalized by the Pt mass. (a) Pt/HMCs-5; (b) Pt/HMCs-10; (c) Pt/HMCs-15; (d) Pt/HMCs-20; (e) Pt (20 wt%)/C; (f)The relationship between peak current density and EG concentrations of different samples. The linear relationships suggest a diffusion-controlled process.

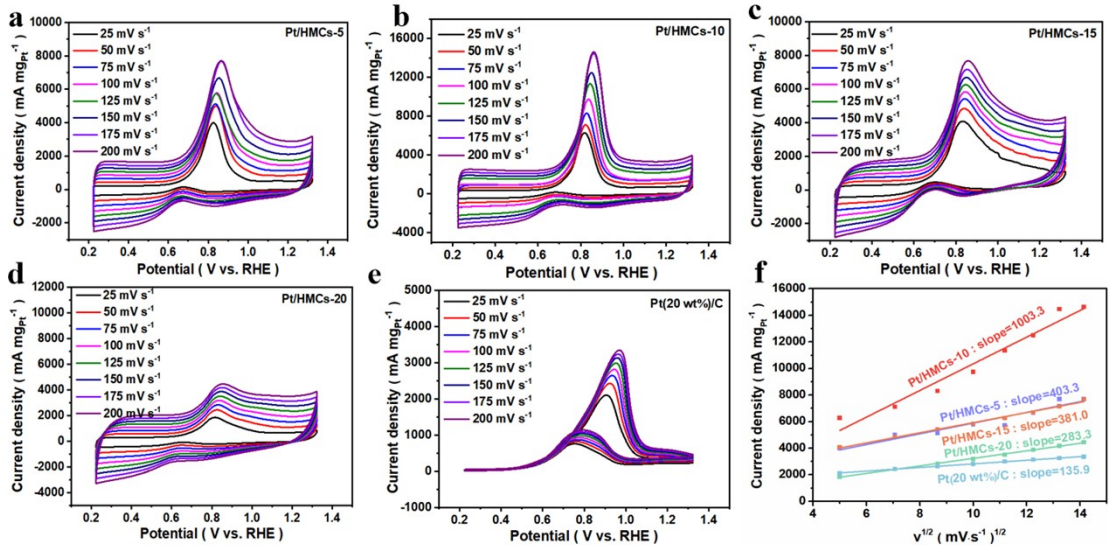

Fig. S18 EGOR curves of as-prepared catalysts at different square root. CV curves of as-prepared catalysts at different scan rates toward EGOR recorded in 1 M KOH electrolyte. The current density is normalized by the Pt mass. (a) Pt/HMCs-5; (b) Pt/HMCs-10; (c) Pt/HMCs-15; (d) Pt/HMCs-20; (e) Pt (20 wt%)/C; (f)The relationship plot between peak current density and square root of scan rate. The linear relationships suggest a diffusion-controlled process.

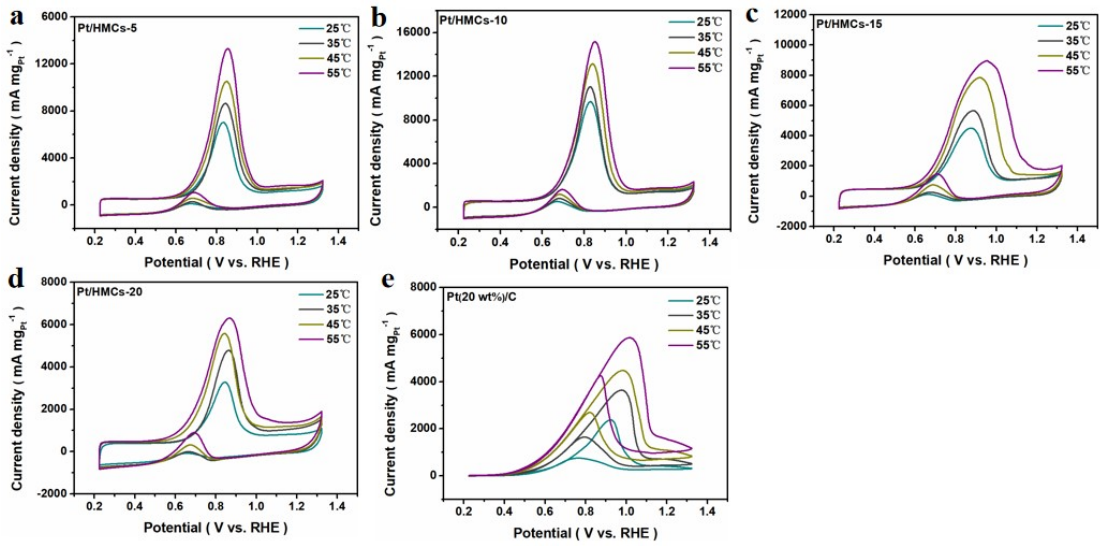

Fig. S19 CV curves of as-prepared catalysts from 298 to 358 K for the EGOR in 1 M KOH + 1 M EG. the scan rate is 10 mV·s^{-1}.

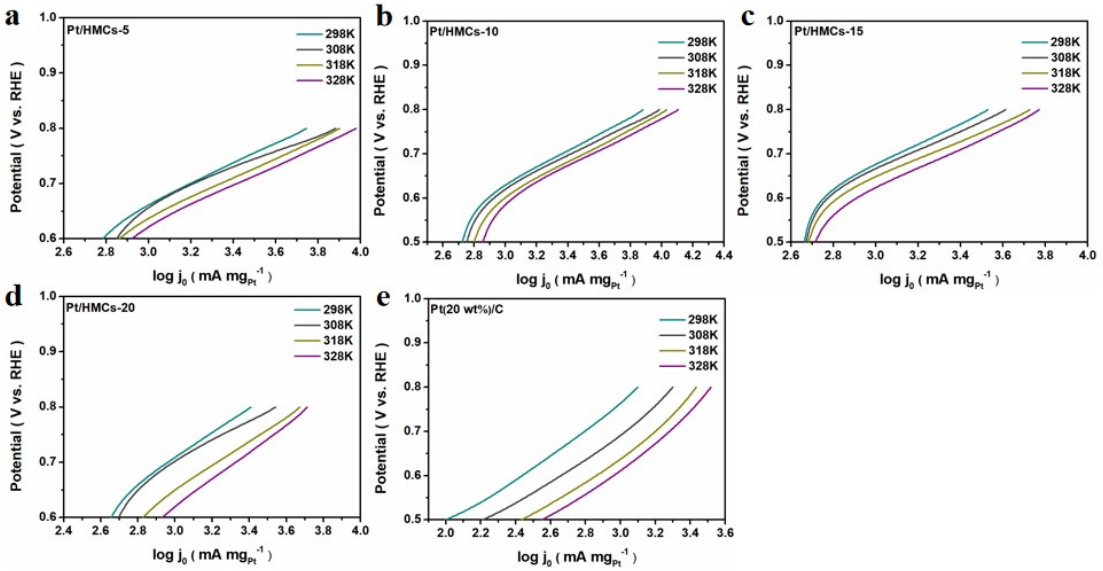

Fig. S20 Tafel curves of as-prepared catalysts from 298 to 348 K for the EGOR.

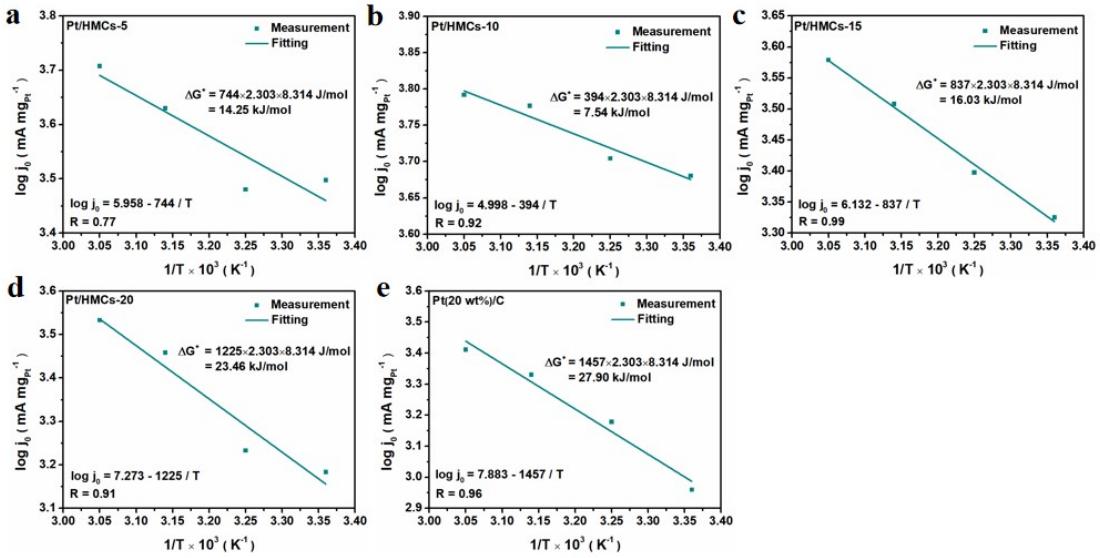

Fig. S21 Typical Arrhenius plots of as-prepared catalysts for the EGOR. The logarithm of the peak current density (log j~p~) from CV curves is plotted against the inverse of temperature (1000/T). The linear fitting of the data allows for the activation free energy (ΔG^x).

Table S4. EGOR performance comparison with recently reported high-performance electrocatalysts.

Catalyst	Pt loading	Electrolyte	Mass activity	Stability	Reference
Pt-Fe alloy	95.8 wt%	1M KOH+1M EG	22.7 A mg^{-1}	50 h	9
PdCu-2 NSs		1M KOH+1M EG	7.545 A mg^{-1}	7200 s	10
Pt_4Rh-L NCs	Pt:Rh=4:1	1M KOH+1M EG	5.13 A mg^{-1}	CVs for 250 cycles	11
$Pt_{52}Cu_{48}$ HTNCs	Pt:Cu=3:1	1 M KOH + 1 M EG	5.7 A mg^{-1}	3600 s	12
$Pd_{58}Cu_{32}Ir_{10}$ NCs	-----	1 M KOH + 1 M EG	4.5 A mg^{-1}	3600 s	13
Pt/HMCs-10	0.83 wt%	1M KOH+1M EG	10.696 A mg^{-1}	7200 s	This work

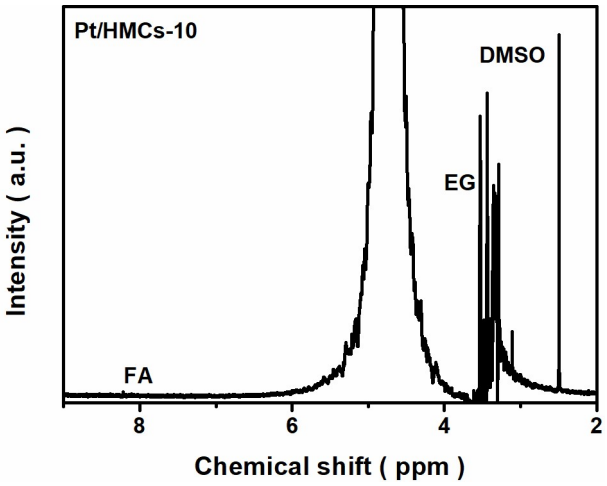

Fig. S22 ^{1}H NMR spectra of the electrolyte after EGOR of Pt/HMCs-10. The electrolyte was collected after chronoamperometric testing at 0.77 V vs. RHE for 2 hours in 1 M KOH + 1 M EG. The characteristic peaks are assigned to formate (HCOOH) at ~8.2 ppm, which is a definitive product of C-C bond cleavage.

Reference

1. D. Liu, X. Li, S. Chen, H. Yan, C. Wang, C. Wu, Y. A. Haleem, S. Duan, J. Lu, B. Ge, P. M. Ajayan, Y. Luo, J. Jiang and L. Song, *Nat. Energy*, 2019, **4**, 512-518.
2. H. He, J. Tian, X. Bai, C. Mao, Y. Zhang, C. Zhou, X. Peng, L. Yang, X. Wang, Q. Wu and Z. Hu, *Science China Materials*, 2025, DOI: 10.1007/s40843-025-3510-0.
3. Y. Guan, Y. Feng, J. Wan, X. Yang, L. Fang, X. Gu, R. Liu, Z. Huang, J. Li, J. Luo, C. Li and Y. Wang, *Small*, 2018, **14**, 1800697.
4. Z. Shi, X. Zhang, X. Lin, G. Liu, C. Ling, S. Xi, B. Chen, Y. Ge, C. Tan, Z. Lai, Z. Huang, X. Ruan, L. Zhai, L. Li, Z. Li, X. Wang, G.-H. Nam, J. Liu, Q. He, Z. Guan, J. Wang, C.-S. Lee, A. R. J. Kucernak and H. Zhang, *Nature*, 2023, **621**, 300-305.
5. T. H. M. Lau, S. Wu, R. Kato, T.-S. Wu, J. Kulhavý, J. Mo, J. Zheng, J. S. Foord, Y.-L. Soo, K. Suenaga, M. T. Darby and S. C. E. Tsang, *ACS Catal.*, 2019, **9**, 7527-7534.
6. C. Li, Z. Chen, H. Yi, Y. Cao, L. Du, Y. Hu, F. Kong, R. Kramer Campen, Y. Gao, C. Du, G. Yin, I. Y. Zhang and Y. Tong, *Angew. Chem. Int. Ed.*, 2020, **59**, 15902-15907.
7. F. Li, D. H. Kweon, G.-F. Han, H.-J. Noh, W. Che, I. Ahmad, H. Y. Jeong, Z. Fu, Y. Lu and J.-B. Baek, *ACS Nano*, 2023, **17**, 2923-2931.
8. H. Wei, K. Huang, D. Wang, R. Zhang, B. Ge, J. Ma, B. Wen, S. Zhang, Q. Li, M. Lei, C. Zhang, J. Irawan, L.-M. Liu and H. Wu, *Nat. Commun.*, 2017, **8**, 1490.

9. H. Lei, N. Ma, K. Li, Y. Wang, Q. Yuan, J. Fan, J. Shui and Y. Huang, *Energy Environ. Sci.*, 2024, **17**, 7792-7802.
10. K. Zhang, C. Wang, H. You, B. Zou, S. Guo, S. Li and Y. Du, *Chem. Eng. J.*, 2022, **438**, 135666.
11. F. Gao, Y. Zhang, P. Song, J. Wang, T. Song, C. Wang, L. Song, Y. Shiraishi and Y. Du, *J. Mater. Chem. A*, 2019, **7**, 7891-7896.
12. H. Xu, P. Song, F. Gao, Y. Shiraishi and Y. Du, *Nanoscale*, 2018, **10**, 8246-8252.
13. C. Chen, T. Song, H. Shang, Q. Liu, M. Yuan, C. Wang and Y. Du, *Int. J. Hydrogen Energy*, 2020, **45**, 26920-26928.